IEEE Access
Multidisciplinary | Rapid Review | Open Access Journal

Received January 3, 2020, accepted January 23, 2020, date of publication January 30, 2020, date of current version February 6, 2020.

Digital Object Identifier 10.1109/ACCESS.2020.2970469

Design of an Integrated Wearable Multi-Sensor Platform Based on Flexible Materials for Neonatal Monitoring

HONGYU CHEN[1,2], SHENJIE BAO[1], CHUNMEI LU[3], LAISHUAN WANG[3], JIANHUA MA[4], PENG WANG[4], HONGBIN LU[4], FENG SHU[5], SIDARTO BAMBANG OETOMO[2,6], AND WEI CHEN[1], (Senior Member, IEEE)

[1]Center for Intelligent Medical Electronics, Department of Electronic Engineering, Fudan University, Shanghai 200433, China
[2]Department of Industrial Design, Eindhoven University of Technology, 5612 Eindhoven, The Netherlands
[3]Children's Hospital of Fudan University, Shanghai 201102, China
[4]Collaborative Innovation Center of Polymers and Polymer Composites, Department of Macromolecular Science, Fudan University, Shanghai 200433, China
[5]Academy of Engineering and Technology, Shanghai Engineering Research Center of UPMCM, Fudan University, Shanghai 200433, China
[6]Department of Neonatology, Máxima Medical Center, 5504 Veldhoven, The Netherlands

Corresponding author: Wei Chen (w_chen@fudan.edu.cn)

This work was supported in part by the National Key Research and Development Program of China under Grant 2017YFE0112000, in part by the Shanghai Municipal Science and Technology Major Project under Grant 2017SHZDZX01, and in part by the Chinese Scholarship Council (CSC).

ABSTRACT For infants admitted at neonatal intensive care unit, the continuous monitoring of health parameters is critical for their optimal treatment and outcomes. So it's crucial to provide proper treatment, accurate and comfortable monitoring conditions for newborn infants. In this paper, we propose wearable sensor systems integrated with flexible material based non-invasive sensors for neonatal monitoring. The system aims at providing reliable vital signs monitoring as well as comfortable clinical environments for neonatal care. The system consists of a smart vest and a cloud platform. In the smart vest, a novel stretching sensor based on Polydimethylsiloxane-Graphene (PDMS-Graphene) compound is created to detect newborns' respiration signal; textile-based dry electrodes are developed to measure Electrocardiograph (ECG) signals; inertial measurement units (IMUs) are embedded to obtain movement information including accelerated speed and angular velocity of newborn wrists. Experiments were conducted to systematically test the sensing related characteristics of the aforementioned flexible materials and the performance of the proposed multi-sensor platform. The results show that the proposed system can achieve high quality signals. The wearable sensor platform is promising for continuous long term monitoring of neonates. The multi-modal physiological and behavioral signals measured by the platform can be further processed for clinical decision support on the neonatal health status.

INDEX TERMS Neonatal monitoring, wearable sensor, flexible materials, electrocardiograph (ECG), respiration.

I. INTRODUCTION

Neonatology is a subspecialty of pediatrics that cares for newborns. Both full-term and preterm infants who suffer from a severe illness during or immediately after birth are admitted to the neonatal intensive care unit (NICU). For babies treated in the NICU, continuous monitoring of vital signs plays a crucial role in providing adequate and timely medical care.

In clinical practice, vital signs for neonatal monitoring in NICU include electrocardiogram (ECG), heart rate, respiration, body temperature and blood oxygen saturation [1], [2]. Traditional monitoring methods usually take accuracy as the first priority, and the comfort of neonates is often overlooked. For instance, ECG signals are acquired by adhesive electrodes, which may cause skin damage and discomfort to newborns [3]. The most commonly used method for detecting respiratory signals is transthoracic impedance detection [4]–[6], which still uses adhesive electrodes to acquire signal in clinical practice. In addition, the detection method

The associate editor coordinating the review of this manuscript and approving it for publication was Venkata Rajesh Pamula.

is susceptible to motion artifacts. Moreover, in a typical NICU environment, the large amount of wires from instruments for collecting vital signs may cause pain and stress on newborns. It is well known that pain and stress negatively impact the brain development of prematurely born infants which may lead to cognitive disturbances and behavioral problems [7].

In recent years, in addition to the data capture technology for processing and decision support [8], different types of wearable sensors and devices, such as accelerometers and gyroscopes, smart fabrics and actuators and wireless communication networks have been developed for clinical research and health monitoring. Health monitoring is an essential application of wearable sensor systems, especially for infants. Together with the advancement of sensor techniques, wearable sensor systems have created a new direction for constant health monitoring of infants. For example, a fully integrated sensory baby vest including sensors for measuring electrocardiography (ECG), respiration, temperature and humidity (used to detect excessive sweating), is developed to detect potential life-threatening events early [9]. Conductive textile wires are used to integrate the sensors into a prototype belt made of soft bamboo fabrics with a negative temperature coefficient (NTC) sensor rather than hard wires to demonstrate temperature monitoring to improve the infant comfort [10]. Bouwstra et al. developed a neonatal smart expandable jacket for newborns, which can measure ECG through textile electrodes. Several experiments were carried out to demonstrate the prototype [11]. Another example is a wearable multi-parameter monitor called BBA bootee, which was developed to monitor infants at significant risk of life-threatening events (ALTE). The sensors, electronics and the power supply are integrated into the bootee to provide reliable pulse oximetry measurements and useful information about the infant's movement and position [12].

Although the aforementioned wearable systems are convenient and the monitoring is continuous, in most of the systems, no systematic verification for the signal quality was carried out. Furthermore, the wearable systems are still limited by an array of problems that severely hinder their performance. For instance, one of the main problems in collecting ECG signals with textile electrodes is the heterogeneity of the skin-electrode impedance. Without buffering, this impedance may seriously distort the ECG data [13]. Another major problem associated with ECG signals using textile electrodes is motion artifact, which refers to the noise in the ECG signal caused by the relative movement between the skin and the electrode. In addition, wearable monitoring methods for respiratory signals also have problems. The feasibility of several sensors in wearable respiratory monitoring systems has been studied: Piezo-sensor or three-dimensional accelerometers signals [14]. However, the respiratory signal collected by piezo-sensors or three-dimensional acceleration sensors contains a large number of motion artifacts, which affect the accuracy of respiratory rate measurements. Proposed by Chadha *et al.* [15], the Respiratory induction plethysmograph (RIP) method consists of an inductive band, that is attached to the abdomen or chest. The resistance of the band varies with stretching. Since the chest/abdominal circumference changes during respiration, RIP - based respiratory monitoring is an effective method for respiratory monitoring. Zhang *et al.* [16], [17] proposed a wearable respiratory monitoring device based on RIP for respiratory biofeedback training. However, the method to produce the band of this device was complicated and difficult to embed in wearable.

In this paper, we develop a monitoring platform embedded with various types of sensors based on flexible materials to acquire ECG, respiratory and motion signals of neonates. The platform is designed to make the clinical detection environment more comfortable and meet the requirements of clinical signal quality. The innovation elements mainly encompass multi-sensor platform design, new flexible material especially for respiration monitoring, the comprehensive verification methods and result analysis of the material, sensors and systems.

In this platform, firstly, a novel stretching sensor based on PDMS-Graphene compound is developed to detect newborns' respiration signal. New material properties and monitoring methods enables the accurate and comfortable monitoring process. Secondly, a convenient electrode structure is proposed in the textile-based dry electrodes which are promising to replace the adhesive electrodes to collect ECG signals in a comfortable way to circumvent possible skin damage. Thirdly, motion signals can be used not only to track movements and optimize the quality of other signals [18]–[20], but also to be served as an important indicator to monitor symptoms such as neonatal seizure [21]–[23]. Thus, we integrated the IMUs into the system for monitoring motion signals.

Furthermore, systematic verification methods are proposed in this work to test the properties of the new materials and sensors as electrodes, as well as to test the signal quality obtained by the new sensor systems. Firstly, for the ECG signal, the electrical properties of different types of textile electrodes are shown based on the same novel structure aiming to achieve the best performance for ECG acquisition. Additionally, statistical analysis and system performance on ECG measurements are conducted under both static and motion conditions. Secondly, for the motion signal, we compared the data gathered by the system with a commercial motion capture system. Thirdly, to prove the feasibility of the new stretching sensor for the respiration monitoring, we presented the basic electrical properties of the new respiration sensor. The results of stability tests and the accuracy of respiration monitoring are reported. Finally, we conducted clinical tests to verify the performance of the proposed monitoring system on 15 neonates from Children's hospital affiliated to Fudan University, Shanghai, China. Given the feasibility that has been confirmed by the pilot study on data collection, transmission and management, the proposed unobtrusive wearable platform is promising to enable the application in both hospital and home-based scenarios.

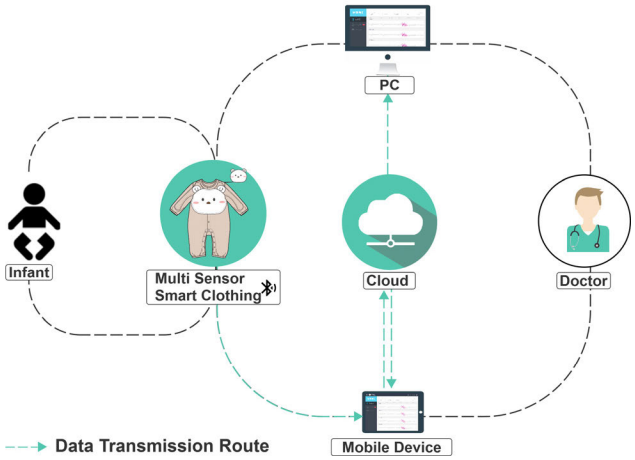

FIGURE 1. System architecture.

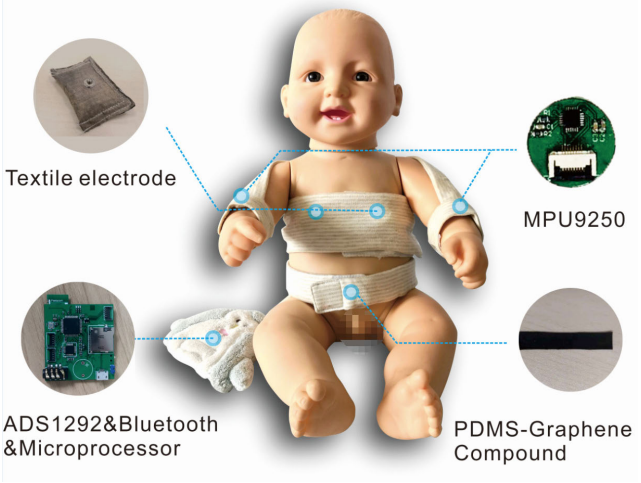

FIGURE 2. Prototype vest.

The rest of the paper is organized as follows: Section II explains the proposed system, including design concepts, prototype implementation and sensors embedded in the system. After that, Section III describes a systematic verification framework for the proposed system. Based on the framework, we will verify ECG, motion and respiration signal by three different kinds of sensors in Section IV, V and VI accordingly. Section VII concludes and discusses the paper.

II. SYSTEM DESIGN

In this section, we illustrate the design concept of an integrated multi-sensor platform and present the prototype, including the hardware, software and the design of novel flexible sensors.

A. DESIGN CONCEPT

The design concept is illustrated in Fig. 1. In the proposed system architecture, a smart vest is proposed with flexible-material based sensors to acquire ECG, motion and respiration signals for newborn infant monitoring non-invasively. The selection of flexible materials for sensors, the fabric of the vest, and the structure of the smart vest have been taken into considerations to achieve high signal quality and better user experience for newborn infants. The data generated by hardware system in smart vest is transmitted to local terminal for real-time monitoring with application. Data will also be uploaded to a cloud platform simultaneously by local terminals. Another control terminal connected with the cloud platform will help doctors to analyze the health status of newborns and provide timely treatments and assistance.

B. PROTOTYPE

In this subsection, the prototype is presented including the platform frame structure, software and the development of new sensors based on the flexible materials.

1) PLATFORM DESIGN

Based on the design conception, a smart vest prototype system integrated with the sensors for ECG, respiration and motion monitoring has been developed as shown in Fig. 2. The proposed vest is made of soft cotton material. PDMS-Graphene compound based sensor, textile electrodes and two IMUs are incorporated into this vest. The data acquisition and processing module of the system is composed of textile electrodes, analog front-end, IMUs, a novel stretching sensor, a microcontroller unit (MCU) and Bluetooth module. This part is mainly achieving the collection, processing, and analysis of bio-signal and motion signal acquisition. The textile electrodes are fixed through an elastic band inside the vest to ensure good contact between electrodes and the skin. The PDMS-Graphene compound based sensor is embedded into a belt inside the vest. IMU sensors are incorporated into the wrist parts of the vest. Then the wireless transmission module sends the data to the terminal, such as mobile and personal computer (PC).

The prototype vest is made of soft solid color cotton fabric. Compared with cotton fabric, materials such as wool, chemical fiber, and nylon may rub babies' skin and generate static electricity, and they could stimulate the skin and reduce human skin's moisture, thus leading to itching. In addition, some artificial fibers are in poor permeability. Therefore, sweat is difficult to be volatilized. So, pure cotton fabric material is a good choice for babies, which suits their skin well for its softness, smoothness and flexibility. The outfits are designed to appear as regular baby clothing aesthetically. The structure of vest is open at the back of body. This structure is easy to wear and remove. For the sensor's stability, the Velcro at the bottom of the sleeves and chest is used to fix the sensors' position. Its shape is a combination of a vest and diaper which is designed because it is simple to fix the whole clothes comparing to non-diaper vests.

2) SIGNAL PROCESSING AND TRANSMISSION

The block diagram of the wireless monitoring system is shown in Fig 3. Graphene compound. One side of the PDMS-G compound tensile sensor is connected to the voltage supply of the circuit and the other side is connected to a 12-bit

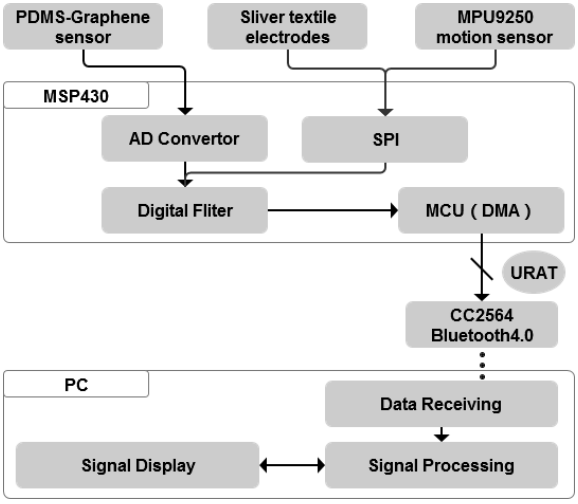

FIGURE 3. Block diagram of the wireless neonatal monitoring system.

analog-to-digital converter (ADC) on the microcontroller unit (MCU) MSP430 (Texas Instruments), with the offset resistor to the ground in the circuit. The output voltage varies according to the resistance of the PDMS-G compound sensor. ECG signals and motion signals were collected by textile electrodes and IMU separately. All the above signal acquisition modules were controlled and managed by the MCU at the sample rate of 500Hz. The timer interruption is called every two microseconds to acquire the signals through a serial peripheral interface (SPI) sequentially. A finite impulse response (FIR) filter is used to control the bandwidth of the data transmission. The filtered signals were sent to the universal asynchronous receiver/transmitter (UART) ports of wireless transmission module (CC2564, Texas Instruments) through direct memory access (DMA) of MSP430. Also, a timestamp is added to the data packet every one second to synchronize the time with that of the medical instruments used in hospitals. The processing procedures can be formulized as a finite state machine (FSM). The data rate in the communication process between the Bluetooth and terminal is 92,000 bits per second.

The overall system is powered by a 3.7V Li-battery, and a charging circuit is designed on the board. The hardware system is designed for low power consumption. From the experiment result, the system can continuously monitor the infant for 8 hours by a 600 mAh battery.

C. SENSOR DESIGN

In this section, we focus on the flexible sensor design and motion sensor integration.

1) PDMS-GRAPHENE COMPOUND FOR RESPIRATION MEASUREMENTS

There exist a variety of methods to detect respiration, mainly covering Acoustic Based Methods, Airflow Based Methods, Chest and Abdominal Movement Detection, Transcutaneous CO2 Monitoring, Electrocardiogram (ECG) Derived Respiration Rate and so on [24]. Among them, mercury strain gauges

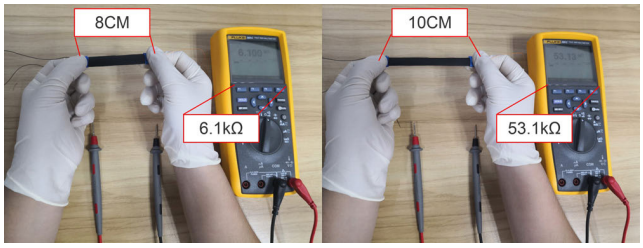

FIGURE 4. Resistance change while PDMS-Graphene compound is stretching. The original state of material (right). The stretched state of material (left).

or impedance methods can be deployed to measure chest and abdominal wall movements [25]. Respiration inductance plethysmography is a non-invasive technique that measures respiration rate through two bands, a thoracic strap placed around the thoracic cage and an abdominal belt placed on the abdomen at the level of the umbilicus. Both were made of extensible/deformable conductive material, extremely fine wire or thin foil that is able to maintain its conductivity during stretching process. The principle of the strain gauge sensor roots in the direct proportion of the resistance and area of the conductor in respiration [22]. In this work, we develop an advanced PDMS-Graphene compound material based sensor and embed the new sensor into clothing to detect newborns' respiration signal.

Since the manufacture process, and composition or ratio of compound affect the resistance, tensile range and sensitivity, in order to obtain materials with large tensile range and high sensitivity, many experiments were conducted for the sensor development. The manufacture process and the ratio of PDMS-Graphene compound in this paper are based on the empirical results. The steps of the fabrication procedure is presented as follows. PDMS, Graphene sheets and xylene were the main raw materials of the PDMS-Graphene compound. 8 g PDMS prepolymer (Sylgard 184, Dow Corning Company, Ltd.), 0.8 g curing agent (Sylgard 184, Dow Corning Company, Ltd.), 1.2 g graphene sheets (Sixth Element (Changzhou) Materials Technology Company, Ltd) were added into a beaker with 60 mL Xylene. Xylene is used to dissolve PMDS prepolymer, which is used as solvent to disperse graphene into PDMS. Then the mixture is bath sonicated for 40 minutes and then stirred for another 3 hours to extensively disperse the graphene sheets. After that, we poured the mixture into a glass plate to evaporate the xylene under ambient conditions and it was ensured that the xylene is completely evaporated. In the end, it was cured at 65 °C in an oven for 3 hours to obtain the final product.

Fig. 4 shows the tensile state and the original state of the new tensile sensor (PDMS-Graphene compound) respectively and demonstrates the feasibility of changing the conductivity of the sensor with the use of a new tool. To better get access to the changes of the abdomen during newborns' respiration, the sensor is designed to be put on the elastic band on the abdomen. Therefore, the length of the elastic band changes with the chest in the process of

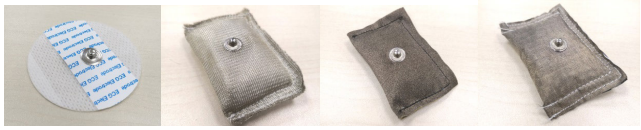

FIGURE 5. AgCl-adhesive ECG electrode (left 1) Textile A (left 2), Textile B (right 2), Textile C (right 1).

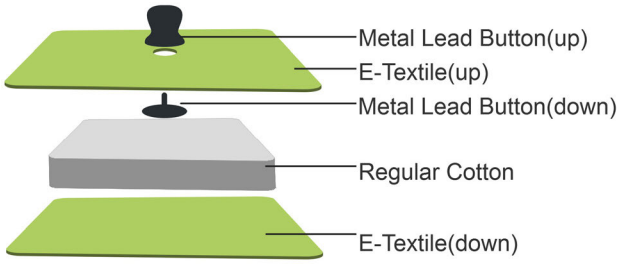

FIGURE 6. Construction of textile electrodes.

newborns' respiration, which helps to extract respiration signals through these changes.

2) FLEXIBLE TEXTILE BASED ELECTRODES FOR ECG MEASUREMENTS

Conductive E-textile material is chosen to obtain ECG signal based on the above mentioned requirements [11]. We developed three types of electrodes with different E-textile materials. Fig. 5 displays proposed three ECG electrodes with different versions. Three different E- textile materials were tested. The model of three textile electrodes are from Balingen, Technik-tex P130 + B and Berlin RS of Shieldex Company and are named as textile A, textile B and textile C. These materials are flexible, non-irritating, lightweight (Balingen :0.062 kg/m^2; Technik-tex P130 + B: 0.135 kg/m^2; Berlin RS:0.055 kg/m^2), thin (Balingen:0.26mm; Technik-tex P130 + B: 0.45mm; Berlin RS:0.11mm), low resistance (Balingen $<$ 0.6ohms/sq; Technik-tex P130 + B $<$ 2 ohms/sq; Berlin RS $<$ 0.5ohms/sq) and convenient to be integrated into the side of the clothing. The values of the parameters of the above textile electrodes were taken from the datasheet [26].

The textile electrode is designed to be disposable, because electrodes will be affected by stains and sweats after use. We put forward a new flexible electrode structure in the proposed system. To ensure the stability of the electrode connection, the connection structure of the flexible electrode is proposed so that the electrode can be replaced, as show in Fig. 6.

The electrode consists of three parts, metal lead button, E-textile and Regular Cotton. E-textile is connected to the metal lead button. Regular Cotton is sandwiched between the E-textile (up) and the E-textile (up), the periphery of E-textiles up and down is stitched by sewing. Motion artifact is one major challenge that textile electrodes face. The proposed sandwich little cushion style of design improve the contact during a relative movement between the electrode and the skin which is perpendicular to the skin, which helps to improve the signal quality during motion.

3) IMU SENSORS FOR MOVEMENT MONITORING

Recently, inertial sensors has been widely used in ambulatory motion analysis [27]. To obtain accurate motion measurements, IMUs, integrating the accelerometers, gyroscopes, and magnetometers are often used.

Thus, in the proposed system, we collected movement signals from two IMUs (Invensense, MPU9250) infant's right wrist and left wrist separately. The placement of IMU module is shown in Fig. 2. The motion signals are transferred to MCU via SPI using Flexible Printed Circuit (FPC) cables.

III. SYSTEM VERIFICATION FRAMEWORK

In this paper, we propose a systematic verification method for wearable hardware system with new materials involved. Fig. 7 shows the framework of evaluation to verify the feasibility of the system by evaluating three kinds of acquisition methods respectively. The targets and methods were designed to objectively verify signal quality from a fundamental aspect to an actual use scenario. For the ECG signal acquired by textile electrodes, we first evaluate the electrical properties of designed electrodes by investigating the skin-to-electrode impedance to promise the signal quality at very beginning. Then statistical indexes as show in table were chosen to assess the signal quality in a standard equipment environment. After the evaluation process of the textile electrodes, they were implemented into the new hardware system, and ECG signals were collected accordingly. Three classical ECG signal quality assessment methods were applied to evaluate ECG signal acquired by proposed system and finally we compare the ECG waveform with the clinical gold standard. Similarly, for the novel stretching sensor based on PDMS-Graphene compound, a feasibility experiment was designed at first. After that, the sensor was embedded in the system for the comparison with a clinical equipment. Moreover, since we use a commercial chip for the motion signal acquisition, the sensor verification method was omitted at this stage and we just compared the signal acquired by the system with commercial Shimmer device.

IV. VERIFICATION OF FLEXIBLE TEXTILE BASED ECG ELECTRODES

A. FLEXIBLE TEXTILE PROPERTIES

1) METHOD

To assess the electrode properties, we set up two experiments. One was to test the skin-to-electrode impedance. The other was the signal quality of the test electrode in the standard equipment environment.

a: SKIN-TO-ELECTRODE IMPEDANCE

The impedance introduced by the skin-to-electrode interface of standard Ag/AgCl electrode and textile electrode were

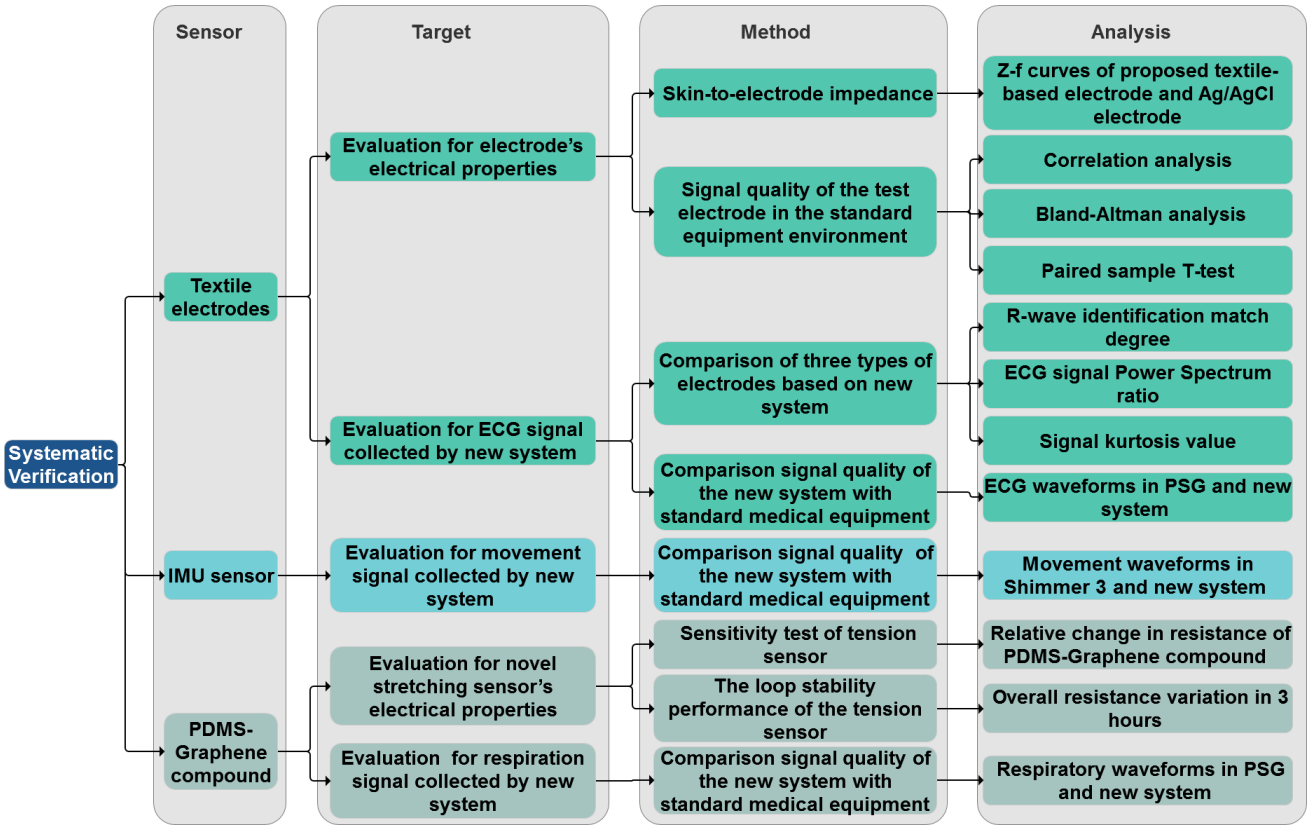

FIGURE 7. Framework for the evaluation.

measured on a person's forearm by an electrochemical workstation (ZAHNER - Zennium).

The two-electrode system was used. Ag/AgCl electrode was deployed as a reference electrode. The work electrodes were chosen from each textile electrode and Ag/AgCl electrode (Covidien, H124SG). The distance between the working electrode and the reference electrode was approximately 9 cm [28]. We fixed the textile electrode with a strap. The frequency of input signal sweeps from 0.1 Hz to 100 kHz. An impedance-frequency curve was drawn for each kind of electrode.

Textile Electrodes Signal Quality Assessment:

We compared the ECG signals acquired by the proposed electrodes and Ag/AgCl electrode (Covidien H135SG) using standard acquisition system.

We collected three sets of data. Each set of data was collected from two different kinds of electrode simultaneously in a static state by shimmer 3 [29], respectively. The study involved a 24-year-old male volunteer. Different electrodes were attached to the adjacent positions on the left and right sides of the subject's chest. The combination of different electrodes was group a: textile A electrode and Ag/AgCl electrode; group b: textile B electrode and Ag/AgCl electrode; group c: textile C electrode and Ag/AgCl electrode. We used shimmer-3 as a standard acquisition device. The acquisition time for each set of data was one and a half hours.

Three statistical analysis methods were conducted to evaluate the signal quality acquired by the novel electrode. Heart rate per minute was extracted by R wave detection algorithm implemented on MATLAB R2018a based on classic QRS detection algorithm proposed by Lee *et al.* [30]. A bandpass filter with passband of 5-15Hz was used to preprocess the data and the hamming window was applied for the function "fir1" in MATLAB. Then a dynamic threshold was determined every five seconds with 2500 values gathered from the system for the "findpeaks" function with the 'MinPeakDistance' index of 150 points which is 0.3 second in the time domain.

Correlation Analysis:

We extracted the average heart rate value per minute and compared the heart rate signals from two different electrodes in each group. Correlation analysis was calculated between heart rate information in each group.

Bland-Altman Analysis:

Similarly, a "Bland-Altman analysis" was performed on the average heart rate of each group.

The standard Ag/AgCl electrode was used as the comparison detection system M1, and the textile electrode was the system M2 to be evaluated. The Bland-Altman analysis was performed to show the difference between heart rate detected by the two systems.

Paired Sample T-Test:

In order to analyze the differences between the signals acquired by textile electrode and standard electrode, a list of

TABLE 1. Selected frequency domain measures of HRV.

Variable	Units	Description
Analysis of short-term recordings (5 min)		
5 min total power	ms²	The variance of normal-to-normal (NN) intervals over the temporal segment
SDNN	ms	Standard deviation of all NN intervals
RMSSD	ms	The square root of the mean of the sum of the squares of differences between adjacent NN intervals
SDSD	ms	The standard deviation of differences between adjacent NN intervals
NN50		Number of pairs of adjacent NN intervals differing by more than 50 ms in the entire recording. T variants are possible counting all such NN intervals pairs or only pairs in which the first or the se interval is longer.
PNN50	%	NN50 count divided by the total number of all NN intervals.
VLF	ms²	Power in very low-frequency range
LF	ms²	Power in the low-frequency range
LF norm	ms²	LF power in normalized units LF/(Total Power–VLF) ×100
HF	ms²	Power in the high-frequency range
HF norm	nu	HF power in the normalized unit HF/(Total Power–VLF) ×100

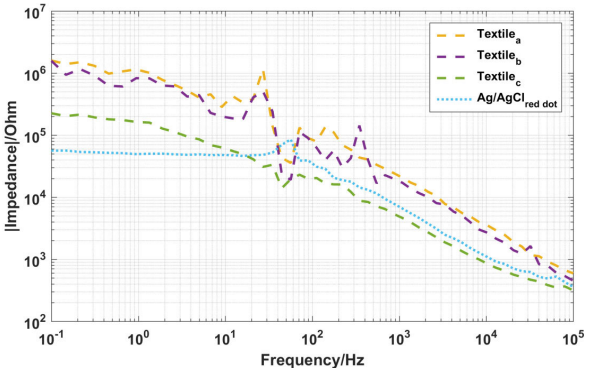

FIGURE 8. Skin-electrode impedance of different electrodes.

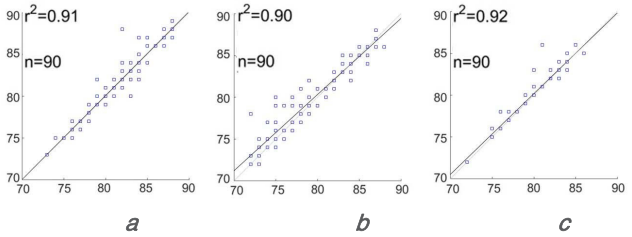

FIGURE 9. Results of Correlation analysis. a. Group A; b. Group B; c. Group C.

physiological parameters shown in Table 1 were compared. These parameters were widely used to characterize the heart rate variability which reflects more fine-grained information about the dynamics of heart activity [31]. Five minutes of continuous ECG were taken as a segment of data, and the data collected for each type of electrode can be divided into 18 segments. Paired T-test was adopted to support our claim that no differences in substance exist between those parameters retrieved from signals acquired by these three kinds of electrode.

2) RESULTS

a: SKIN-TO-ELECTRODE IMPEDANCE

Fig.8 gives the Z-f curves which characterize the skin-to-electrode interface of the proposed textile-based electrode and Ag/AgCl electrode (Covidien, H124SG) respectively. The frequency ranges from 0.1 Hz to 100 kHz. Test results demonstrate that the impedance introduced by skin-to-electrode interface also decreases as the frequency of stimulus signal increases. In the frequency range of most bio-potential signals, the impedance corresponding to textile C-based electrode was the smallest (∼500 kOhm in near dc range) while the impedance corresponding to textile A-based was the largest (∼725 kOhm in near dc range). The impedance corresponding to Ag/AgCl electrode was slightly larger than that of textile C-based electrode, about 575 kOhm in near dc range. The significances of all data points were all larger than 0.95.

b: TEXTILE ELECTRODES SIGNAL QUALITY ASSESSMENT

① Correlation analysis results

We extracted heart rates and did a correlation analysis and Bland-Altman analysis. Fig. 9 shows the results of the correlation analysis of the three sets of data. Correlation analysis results showed that the R^2 values of the three A, B, C groups were all within the range of 0-1, and the R-value of the C electrode was the largest, 0.92. Therefore, the signals collected by the three textile electrodes were positively correlated with the signals acquired by the standard electrodes.

② Bland-Altman analysis results

Fig. 10 shows the results of Bland-Altman analysis. It can be seen in Fig. 10-a that the 95% consistency limit was (2.3, −2.1); the 3% point was beyond the 95% consensus limit; the M1 and M2 systems the absolute value of the difference between the measured values is Y at the maximum; the average of both systems was 0.40. As can be seen in Fig. 10-b, the 95% consistency limit was (3.1, −2.3); the 2% point was 95% beyond the consensus limit; the absolute value of the difference between the M1 and M2 system detection

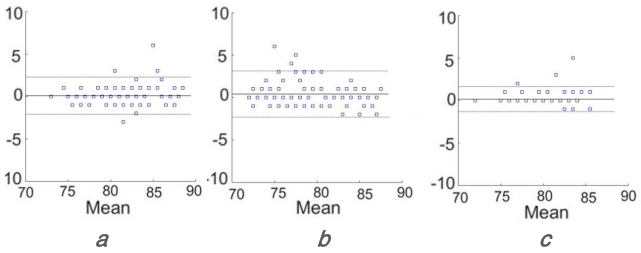

FIGURE 10. Results of Bland-Altman analysis.

TABLE 2. T-test results of Group A, B, C.

Variable	Statistical significance (Group A)	Statistical significance (Group B)	Statistical significance (Group C)
5 min total power	0.525	0.500	0.700
NN50 (M1) - NN50 (M1)	0.660	0.106	0.072
PNN50 - PNN50(M1)	0.598	0.105	0.071
SDNN	0.529	0.501	0.460
RMSDD	0.596	0.370	0.306
SDSD	0.606	0.349	0.311
VLF(M1)- VLF(M1)	0.782	0.185	0.922
LF(M1)- LF(M1)	0.606	0.186	0.990
LF norm(M1)- LF norm(M1)	0.510	0.852	0.015
HF(M1)- HF(M1)	0.938	0.396	0.484
HF norm(M1)- HF norm(M1)	0.067	0.577	0.072

values was Y; The average system result was 0.41. It can be seen in Fig. 10-c that the 95% consistency limit was (1.6, −1.3); the 2% point was 95% beyond the consensus limit; the absolute value of the difference between the M1 and M2 system detection values was Y; The average of the system results was 0.10. It can be seen from the results that the three groups of textile electrodes have a good agreement with the standard Ag/AgCl electrodes, and the average value of the results in group C was closest to zero.

③ Paired sample T-test results

The results are shown in the Table 2. The results show that the significance values of each indicator of three kinds of electrodes are all greater than 0.05.

Therefore, there are no differences between the indicators of the ECG signals collected by the three textile electrodes and the standard electrodes.

B. ECG SIGNAL COLLECTED BY PROPOSED SYSTEM

1) METHOD

a: COMPARISON METHOD OF THREE TYPES OF ELECTRODES BASED ON PROPOSED SYSTEM

After the experiment of electrode's electrical properties, the electrodes were evaluated to acquire ECG signal. For performance evaluation of the textile electrode using proposed system, ECG signals were measured in different human body motion states in a 24-year-old male volunteer. Two electrodes were fixed on the left and right sides of the ribcage of each test subject. To ensure similar test conditions for comparison, these electrodes were positioned in the same locations for every measurement. The sitting-state ECG signals were measured first, and then the motion artifacts that result from walking and upper body turning of the subject's arms were investigated Test time of each group was 2 minutes.

We use following three indicators as the evaluation of signal quality factors which are the critical facts in the further research. These indicators are shown below:

R-Wave Identification Match Degree:

Using the same heart rate detection method aforementioned, we define the R-wave matching degree M(ω) as

$$M(\omega) = \frac{N(\omega)}{N_A(\omega)} \tag{1}$$

whereby N (ω) is the number of R waves matched by the algorithm, and NA (ω) is the number of R waves manually counted by experts.

We chose this specific preprocessing and R wave detection method to minimize the effect of the algorithm thus to verify the amplitude of ECG signals acquired by different types of electrodes under same movement.

ECG Signal Power Spectrum Ratio:

According to Donald et al. and others [32], [33], QRS complex mainly concentrates in the 2∼20Hz, powerline is in 50 or 60Hz, the baseline drift is in 0.15∼0.3Hz [34]. The main energy of QRS wave concentrates at 12Hz [35], and ECG signal is subject to motion artifacts and EMG interference between 3∼30Hz [30]. So in this paper, the ratio of ECG signal power density between 5∼15Hz and 3∼30Hz is calculated to estimate the state of motion ECG signal quality.

$$S(\omega) = \frac{\int_5^{15} P(\omega)d\omega}{\int_3^{30} P(\omega)d\omega} \tag{2}$$

P (f) denotes the power spectrum of ECG signal.

Signal Kurtosis Value:

ECG signals are collected as discrete signals. According to the central limit theorem, the kurtosis of the discrete signal reflects the Gaussian of the signal.

$$K = \frac{1}{M}\sum_{i=1}^{M}\left[\frac{x_i - \mu_x}{\sigma}\right]^4 \tag{3}$$

μ_x denotes the mean of the signal xi, σ denotes the standard deviation of the signal, and M is the number of sampling points of the measured data segment.

The corresponding level of the ECG signal quality evaluation is presented in table 3.

b: COMPARISON METHOD OF THE PROPOSED SYSTEM WITH STANDARD MEDICAL EQUIPMENT

After obtained experiment results about the flexible electrodes proposed, we used PSG (Polysomnography) as

TABLE 3. Signal quality factors.

Signal quality factors	Good	Normal	Bad
R-wave matching degree (M)	M⩾0.8	0.8>M⩾0.6	0.6>M
Power Spectrum ratio (S)	S⩾0.5	0.5>S⩾0.4	0.4>S
Signal Kurtosis (K)	K>5	5>K⩾4.3	4.3>K

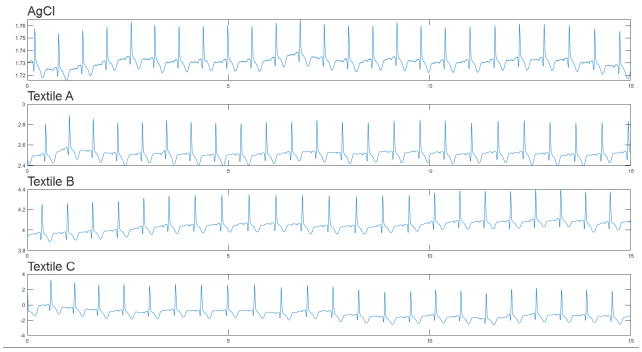

FIGURE 11. R-wave Recognition under sitting state.

TABLE 4. R-wave Recognition under sitting state.

Type of electrode	AgCl	Textile A	Textile B	Textile C
Missed	0	0	0	0
N (ω) Identified by algorithm	161	167	173	171
NA (ω)Detected by experts	161	167	173	171
R-wave matching degree (M)	1	1	1	1

gold standard to compare the waveform in this experiment. According to the preliminary experimental results, we selected textile C materials to compare the ECG waveform with PSG and compared the ECG signals acquired by our system with textile C electrodes and PSG with AgCl electrodes. Altogether six electrodes were fixed on the volunteer simultaneously with an experiment time of five minutes.

2) RESULTS

a: COMPARISON RESULT OF THREE TYPES OF ELECTRODES BASED ON PROPOSED SYSTEM

To analyze the electrode performance under motion artifacts, the measurements were performed in sitting state, upper body turning state and walking state.

Sitting State Results:

QRS wave group and T wave can be detected obviously under the sitting state. The results of R-waves detection are presented in Fig. 11 and Table 4. R-wave recognition rate was generally high, and there was a small difference among three kinds of textile electrodes. Power spectrum ratio and signal kurtosis values of 1000 points selected during the test time of two minutes were listed in Table 5 and 6. The S and K values of the three textile electrodes and the Ag/AgCl electrodes

TABLE 5. Power spectrum of ECG under sitting state.

Type of electrode	AgCl	Textile A	Textile B	Textile C
Power Spectrum ratio (S)	0.7407	0.7291	0.7283	0.7709

TABLE 6. Signal quality under sitting state.

Type of electrode	AgCl	Textile A	Textile B	Textile C
Signal Kurtosis (K)	10.3668	9.8756	7.4843	11.2188

TABLE 7. R-wave Recognition under turning stat.

Type of electrode	AgCl	Textile A	Textile B	Textile C
Missed	0	1	6	0
False alarm	0	0	0	0
N (ω) Identified by algorithm	201	186	191	181
NA (ω)Detected by experts	201	187	197	181
R-wave matching degree (M)	1	0.994	0.97	1

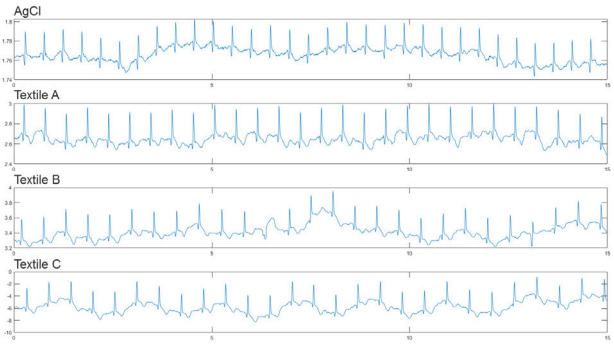

FIGURE 12. R-wave Recognition under sitting state.

TABLE 8. Power spectrum of ECG under turning state.

Type of electrode	AgCl	Textile A	Textile B	Textile C
Power Spectrum ratio (S)	0.8481	0.7051	0.6477	0.7039

were all in good level. The S and K values of textile C electrode were better than those of Ag/AgCl electrode.

Upper Body Turning State Results:

Detection data of QRS wave and T wave were displayed in Table 7 and Fig. 12. Power spectrum ratio and signal kurtosis values during the sitting state were listed in Table 8 and 9.

Compared with sitting state, ECG signal was more prone to drift in upper body turning state. According to the signal quality factors in Table 3, the results showed that the values of K, S and M of the AgCl electrode and the textile electrode C were all at a good level. The K values of the textile electrodes A and B are at the normal level.

TABLE 9. Signal quality under turning state.

Type of electrode	AgCl	Textile A	Textile B	Textile C
Signal Kurtosis (K)	8.2667	4.7987	4.9923	7.4293

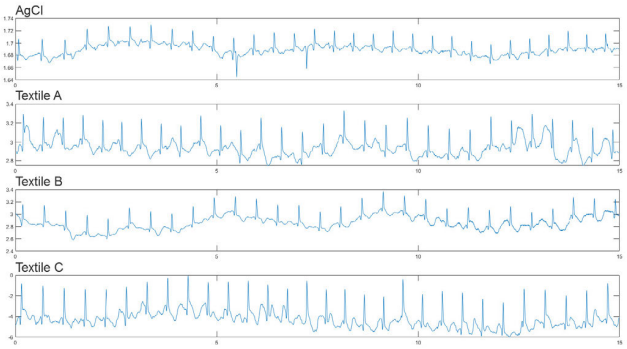

FIGURE 13. R-wave Recognition under walking state.

TABLE 10. R-wave Recognition under walking state.

Type of electrode	AgCl	Textile A	Textile B	Textile C
Missed	3	21	7	1
False alarm	0	0	2	0
N (ω) Identified by algorithm	205	193	204	202
NA (ω)Detected by experts	208	214	209	203
R-wave matching degree (M)	0.986	0.901	0.976	0.995

TABLE 11. Power spectrum of ECG under walking state.

Type of electrode	AgCl	Textile A	Textile B	Textile C
Power Spectrum ratio (S)	0.6386	0.3603	0.4223	0.4119

TABLE 12. Signal quality under walking state.

Type of electrode	AgCl	Textile A	Textile B	Textile C
Signal Kurtosis (K)	9.1456	6.7123	5.0471	7.1517

Walking State Results:

Table 10 and Fig. 13 show the ECG waveforms collected from different electrodes under the walking state. Power spectrum ratio and signal kurtosis values are listed in Table 11 and 12. Like the upper body turning state, the ECG signal was prone to drift in the walking state. In the state of walking, the M value of textile electrode C was the largest. The K and S values of the three textile electrodes were not as good as those of the AgCl electrodes. However, the K and M value of textile electrode B and C reached a good level.

Three indexes of R-wave recognition, power spectrum ratio, and signal kurtosis value were used to make a comprehensive evaluation of electrodes under each state. According to these indexes, the performance of AgCl-adhesive was the best, and textile electrode C was better than A and B.

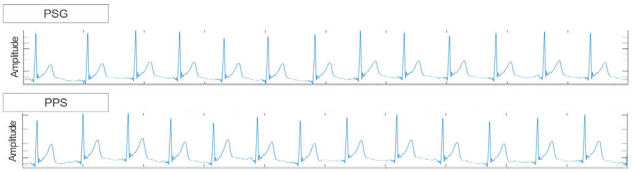

FIGURE 14. ECG signal collected by proposed system and PSG.

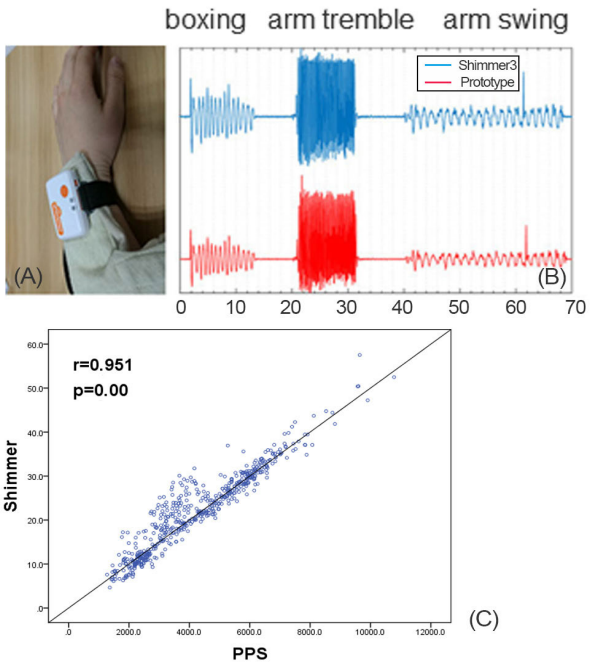

FIGURE 15. Motion signal experimental setup (A) Motion signal waveforms (B) Results of Correlation analysis (C).

b: COMPARISON RESULTS OF THE PROPOSED SYSTEM WITH STANDARD MEDICAL EQUIPMENT

ECG waveforms acquired by the proposed system and PSG under static state were given in Fig. 14. We can see that the smart vest can acquire ECG signals of comparable signal quality with respect to PSG.

V. IMU SENSOR VERIFICATION

A. METHOD FOR MOTION SIGNAL COLLECTED BY PROPOSED SYSTEM

Experiments on adults were carried out to validate the motion analysis part of our system. The prototype and Shimmer 3 were attached to the left wrist as was shown in Fig. 15-A.

A standard protocol was followed, where different types of movements, including boxing, arm swing, arm tremble etc.

B. RESULTS

Fig. 15-B shows the comparison of the mean square values of 3-axis accelerations, which demonstrates that the IMU data measured by the prototype has the comparable data quality of the commercial shimmer device. Fig. 15-C shows the correlation analysis for the readings obtained from the PPS.

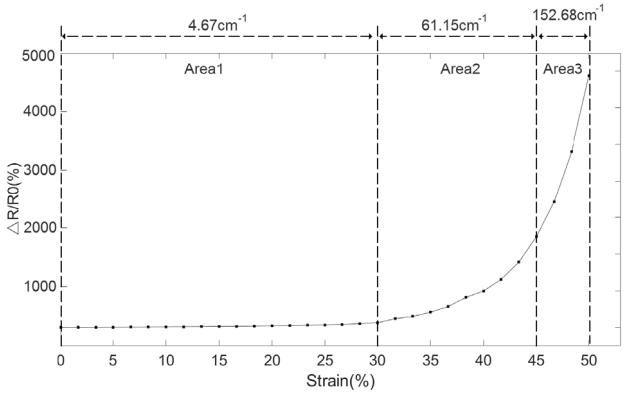

FIGURE 16. Relative change in resistance of PDMS-graphene compound versus strain within strain range of 0-50%.

The vertical axis represents the reference reading given by Shimmer 3, and the horizontal axis represents the values provided by the PPS for the corresponding time segments. The PPS was found to have a Pearson correlation(r) of 0.951 with the reference values.

VI. RESPIRATION SIGNAL VERIFICATION

A. PDMS-GRAPHENE COMPOUND PROPERTIES

1) METHOD

The method of obtaining the abdominal respiration signal by stretching the sensor mainly involves resistance change caused by the stretching of this material. Therefore, we tested the sensitivity and cycle stability of PDMS-Graphene compound. The initial resistance of this sample sensor is approximately 85kΩ with the original length of about 35cm and after stretching it to 42cm length, the resistance of it will rise to 320kΩ correspondingly. In order to test the properties of materials, we set up the following two experiments.

a: SENSITIVITY TEST OF TENSION SENSOR

In this experiment, multi-meter (FLUKE) was used to measure the change of the resistance of the sensor under different lengths. We fix the ends of the material and change the length of the sensor by stretching it. Our test deformation range was 0-70%.

b: THE LOOP STABILITY PERFORMANCE OF THE TENSION SENSOR

We tested the loop performance of the sensor by using a stepping motor to control the movement on a screw rod. The stretch length was stable with the frequency of 20 cycles per minutes which was similar with the normal respiration frequency. A resistance-voltage circuit and ADC on Arduino was used to gather the digital signal and the data was transmitted through UART and stored on the local terminal. The duration of the loop stability test was 3 hours.

2) RESULTS

Fig. 16 shows the relative change in resistance for various elongation values. We found no linear behavior of the sensor, but we could identify three different areas of the sensitivity. In the first area, elongation of the sensor was from 8 cm to 10.4cm, the sensitivity was 4.57 cm−1.In the second area, elongation the sensor from 10.4 cm to 11.6 range, the sensitivity was 61.15 cm−1, and the third area showed a further increase of the sensitivity to 152.68 cm−1 when the sensor was fully stretched to 12 cm.

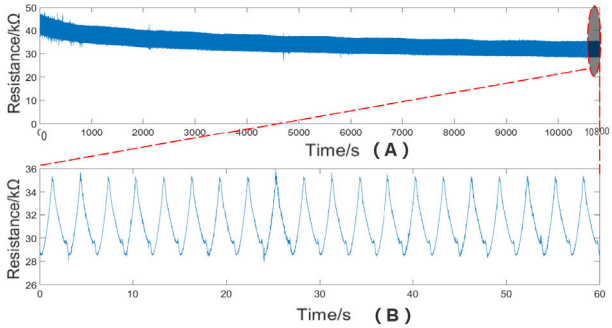

FIGURE 17. Results of the three hours' stability test (A) overall resistance variation in 3 hours (B) detailed waveform in the last 1 minute of the whole test.

We noticed that within 30% strain, the graphene-based coated fiber sensors with varying strain presented highly coincident "(ΔR/R0)/ ΔL" strain value. In the strain of 30% to 50% range, "(ΔR/R0)/ ΔL" strain value gradually rises. This range was actually the range of changes that need to be achieved when the elastic band was connected to the body.

For stability testing, Fig. 17-A shows the 3-hour stability test results, and Fig. 17-B shows a portion of the results for the last 1 minute. From these diagrams, we can conclude that the baseline of the whole test period declined gently, but the results of cyclic test were relatively stable after 3,600 cycles of 3 consecutive hours. The slow decline in baseline does not affect the measurement of respiratory signals compared to the range of variation created by measurement of respiration. The detailed waveform of the last 1 minutes signal shows good signal quality. Detecting changes in abdominal circumference was an important feature that can be monitored over a long period of time.

B. RESPIRATION SIGNAL COLLECTED BY PROPOSED SYSTEM

1) METHOD

To assess the basic monitoring performance of proposed system (PPS), we compared our system with the RIP module as part of the PSG apparatus, when both systems were installed on the subject for simultaneous recording of respiration. The respiratory band used in PSG was based on inductance change formed by the coil inside the band. As shown in Fig. 18, PSG respiratory detection band was attached to the abdomen, and PDMS-graphene tensile sensor was attached lower than PSG band. PSG has a respiration sampling frequency of 32Hz.

First of all, we compare the respiration signals acquired by the PPS and PSG to perform a visual comparison. We compare the similarity of the original waveform output of the PPS and the PSG.

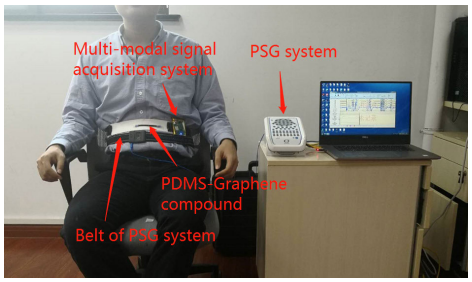

FIGURE 18. Respiratory signal experimental setup.

The second outcome measure for the study was mean difference in average RR between propose system and PSG. Each RR point was output for a 30 second interval. The secondary outcome was the correlation analysis between the respiratory rates measured for PPS and PSG.

The difference in average RR between monitoring techniques over this 30 second interval was summarized using the mean, standard deviation, median and range. The effectiveness of the PPS monitor versus PSG-derived RR was determined by 95 % confidence intervals for the mean difference in average RR between techniques. A difference of three breaths per minute (bpm) was considered of minimum clinical relevance. This was chosen from the early warning system (EWS) which identifies a score difference of 3 bpm to be meaningful by defining the respiration scores in steps of no greater than 3 bpm.

The third analysis was to assess the direct relationship or correlation between the measured respiratory rate for the PPS device and each of the examined measuring techniques. A Pearson's Bland-Altman analysis was performed.

The PPS would be considered effective in detecting changes in RR comparable to PSG if a correlation coefficient (r) greater than 0.8 was achieved. The expected correlation with PSG-derived RR was set at 0.8 because the continuous nature of both the PPS and PSG-derived monitoring could be expected to result in a higher correlation. Bland-Altman analysis was used to present the results graphically.

2) RESULT

The experiment was carried out on a 30-year-old male volunteer for 4 hours. The subjects sat in a chair without strenuous exercise, during the trial. Firstly, we compare the signal quality in time domain, as show in Fig. 19. From Fig. 19, we see that the signals obtained using the PPS show the similar beat structure of the same frequency with those of the PSG. Though the attaching positions of the PPS and the PSG were a little different from each other in the abdomen region, the overall similarity of the data obtained during the inspiratory intervals can be noted implying the accuracy of the PPS in measuring the breathing rate.

Secondly, of the total 160 recorded data points, each RR point was spaced one minute apart to ensure variable independence in Bland–Altman analysis. 154 time points were available for analysis. The remaining 6 time points were lost

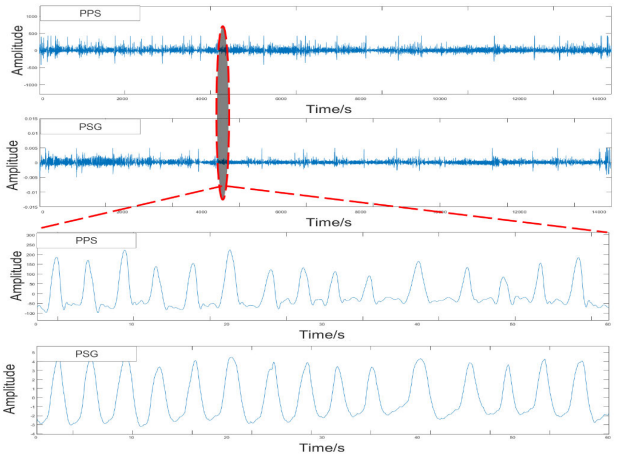

FIGURE 19. Signals measured by PPS and PSG.

TABLE 13. Comparison of average respiratory rate in breaths per minute between PPS and PSG.

PPS-PSG	
Number of data points	*154*
Mean	*-0.15*
Standard deviation	*0.86*
Minimum–maximum	*-4.26,3.10*
95 % confidence interval	*-1.84,1.55*

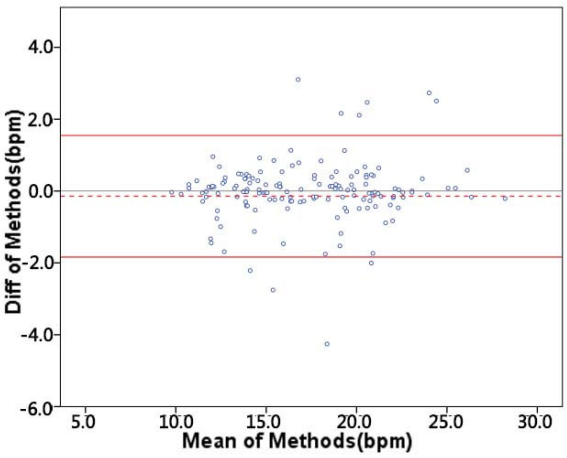

FIGURE 20. Bland-Altman plot showing PPS versus PSG. Direction of difference was (PPS-PSG).

due to the PSG wire falling off when the subject left the chair to rest. Comparisons of the PPS with PSG-derived RR were presented in Table 13. Fig. 20 summarizes the data from the utilized 154 epochs for PSG versus PPS in the form of a Bland–Altman plot. The direction of difference is: (PPS–PSG). The red dashed line represents the bias of the differences. Red solid lines represent the 95 % confidence limits for the differences. The mean difference for average RR between PPS and PSG was less than 1 bpm, mean (SD) = −0.15 (0.86). The 95 % confidence interval (CI) for the difference in average RR was calculated to be [−1.84, 1.55], which does not exclude the clinically relevant difference

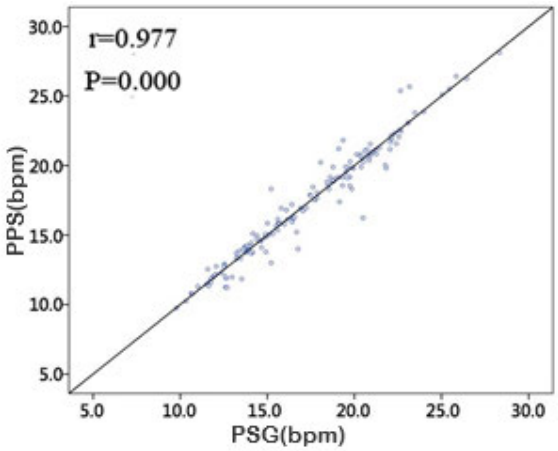

FIGURE 21. Results of Correlation analysis.

of 3 bpm. However, the difference was greater than 3 bpm in the case of just two intervals (1.3 % of intervals).

Finally, Fig.21 shows the results of the correlation analysis of the data from the utilized 154 epochs for PSG versus PPS. The Pearson Correlation (r) of 0.977 demonstrates a very strong relationship between PPS and PSG in monitoring RR.

VII. CLINICAL TEST IN NEONATAL

A. METHOD

After the performance tests on adults, permission was obtained from the Children's Hospital affiliated to Fudan University Research Ethics Committee (approval No. (2017) 89) to recruit infant patients for multi signal monitoring. Inclusion criteria were: age under 60 days, in stable health conditions, about to discharge from neonatal intensive care unit (NICU). Exclusion criteria were: patients with diagnosed respiratory disorders history and allergy to medical grade skin adhesive or latex.

15 patients who did not violate our exclusion criteria were enrolled in the experiments. The mean age of the subjects was 36 days (median 33, standard deviation 12.5, range 18-59). Seven male and eight female subjects were recruited. The average data collection time per subject was 10 min. No adverse respiratory events and skin allergy occurred during the test. The subjects lie in an incubator and keeps awake during the trial.

We compared our system with the PSG, when both systems were attached on the subject for simultaneous recording of ECG and respiration, as show in Fig22. Data analysis methods including visual comparison, and accuracy analysis.

B. RESULT

First we compared the ECG and respiration signal quality in time domain. ECG waveforms acquired by PSG and PPS were given in Fig. 23. The figure shows that the proposed electrode can acquire ECG signals of comparable signal quality and amplitude (thus, also average power) with respect to PSG. The respiration signal quality in time domain was

FIGURE 22. Signals measured by new system and PSG.

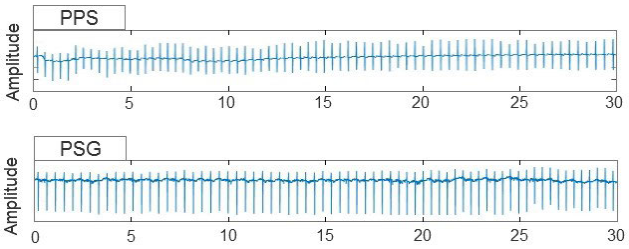

FIGURE 23. Clinical ECG data measured by PPS and PSG.

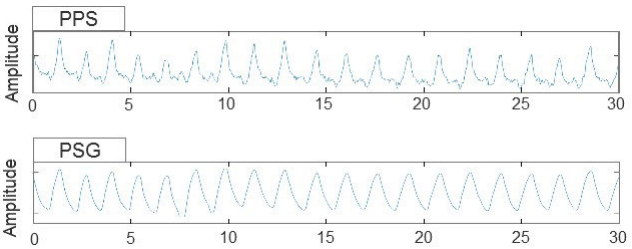

FIGURE 24. Clinical respiration data measured by PPS and PSG.

compared also, as shown in Figure 24. As shown in Figure24, the signal with the same beat frequency structure can be obtained by using PPS and PSG. Although PPS and PSG have slightly different attachment locations in the abdominal region, the overall similarity of the data obtained during the inspiratory interval can be noted.

The second outcome measurement for the study was correlation in average heart rate (HR) and average respiratory rate (RR) between the proposed system and PSG. A total of 150 HR data point and 150 RR data point, Each HR and RR point was output for a 60 second interval. Fig. 25 shows the correlation analysis for the HR obtained from the clinical study. Vertical axis represents the reference reading given by the PSG and the horizontal axis represents the results given by the PPS for the corresponding time segments. The value of Pearson correlation(r) between PSG and PPG in HR monitoring was 0.967. Fig. 26 shows the correlation analysis for the RR obtained from the clinical study. Vertical axis represents the reference reading given by the PSG and the horizontal axis

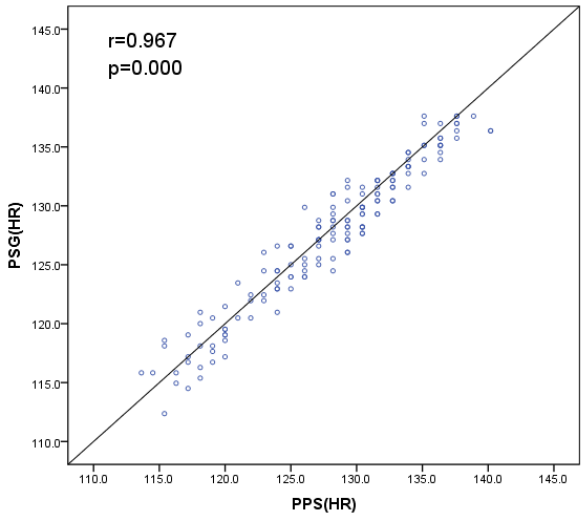

FIGURE 25. Correlation regression analysis for the results obtained from the heart rate clinical data collection exercise.

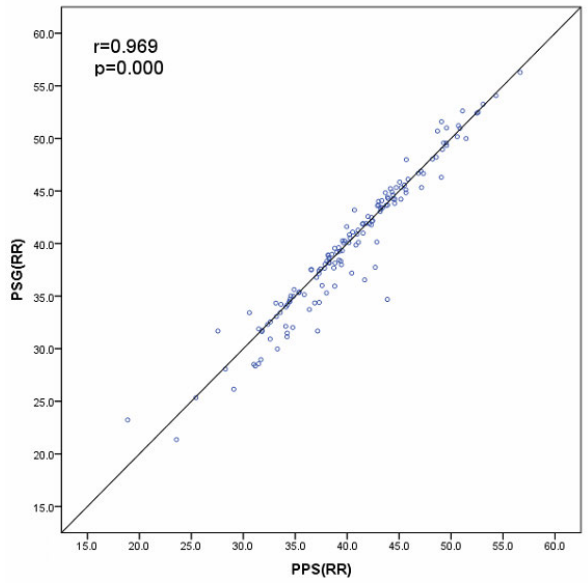

FIGURE 26. Correlation regression analysis for the results obtained from the respiration rate clinical data collection exercise.

represents the results given by the PPS for the corresponding time segments. The value of Pearson correlation(r) between PSG and PPG in RR monitoring was 0.969. The r value of HR and RR demonstrate a very strong relationship between PPS and PSG in monitoring HR and RR.

VIII. CONCLUSION AND FUTURE WORK

In this paper, we propose a smart vest as a unified sensing platform embedded with flexible material based non-invasive sensors for neonatal monitoring. We carried out systematic verification about the platform which includes electrical properties of the new sensing materials, signal quality evaluation and comparison with gold standard to verify the feasibility of the system. Verification experiments prove that quality ECG signals can be obtained through the proposed flexible electrode materials with comparable performance to the commercial AgCl adhesive electrodes and accurate respiration data can be obtained through new PDMS-Graphene compound based stretching sensor. The proposed platform is promising to provide comfort experience during neonatal monitoring.

For future work, we will further improve the structure and electronic properties of the innovative materials to enhance the stability of the measured signal, especially during motion. Furthermore, we will conduct more clinical trials to verify the performance of the wearable platform. Data fusion techniques and optimization algorithms will be explored with the help of clinical data.

The system is ambitious to serve as an effective auxiliary monitoring and diagnostic method to the benefit of existing condition for clinical decision support. Given the characteristics mentioned above, it is also potential in fields like general movement assessment (GMA), early intervention and home monitoring.

REFERENCES

[1] S. H. Abman, W. W. Fox, and R. A. Polin, *Fetal and Neonatal Physiology*. 2004.

[2] H. Als, "Individualized behavioral and environmental care for the very low birth weight preterm infant at high risk for bronchopulmonary dysplasia: Neonatal intensive care unit and developmental outcome," *Pediatrics*, vol. 78, no. 6, pp. 1123–1132, Dec. 1986.

[3] H. Chen, X. Gu, Z. Mei, K. Xu, K. Yan, C. Lu, L. Wang, F. Shu, Q. Xu, S. B. Oetomo, and W. Chen, "A wearable sensor system for neonatal seizure monitoring," in *Proc. IEEE 14th Int. Conf. Wearable Implant. Body Sensor Netw. (BSN)*, May 2017, doi: 10.1109/bsn.2017.7935999.

[4] S. Kano, Y. Dobashi, and M. Fujii, "Silica nanoparticle-based portable respiration sensor for analysis of respiration rate, pattern, and phase during exercise," *IEEE Sens. Lett.*, vol. 2, no. 1, pp. 1–4, Mar. 2018, doi: 10.1109/lsens.2017.2787099.

[5] P. J. Lee, "Clinical evaluation of a novel respiratory rate monitor," *J. Clin. Monit. Comput.*, vol. 30, no. 2, pp. 175–183, Apr. 2016, doi: 10.1007/s10877-015-9697-4.

[6] P. B. Lovett, J. M. Buchwald, K. StÜrmann, and P. Bijur, "The vexatious vital: Neither clinical measurements by nurses nor an electronic monitor provides accurate measurements of respiratory rate in triage," *Ann. Emergency Med.*, vol. 45, no. 1, pp. 68–76, Jan. 2005, doi: 10.1016/j.annemergmed.2004.06.016.

[7] H. Als, L. Gilkerson, F. H. Duffy, G. B. Mcanulty, D. M. Buehler, K. Vandenberg, N. Sweet, E. Sell, R. B. Parad, S. A. Ringer, S. C. Butler, J. G. Blickman, and K. J. Jones, "A three-center, randomized, controlled trial of individualized developmental care for very low birth weight preterm infants: Medical, neurodevelopmental, parenting, and caregiving effects," *J. Developmental Behav. Pediatrics*, vol. 24, no. 6, pp. 399–408, Dec. 2003.

[8] M. Chan, D. EstÈve, J.-Y. Fourniols, C. Escriba, and E. Campo, "Smart wearable systems: Current status and future challenges," *Artif. Intell. Med.*, vol. 56, no. 3, pp. 137–156, Nov. 2012, doi: 10.1016/j.artmed.2012.09.003.

[9] C. Linti, H. Horter, P. Osterreicher, and H. Planck, "Sensory baby vest for the monitoring of infants," in *Proc. Int. Workshop Wearable Implant. Body Sensor Netw. (BSN)*, Apr. 2006, p. 3 and 137, doi: 10.1109/bsn.2006.49.

[10] W. Chen, S. Dols, S. B. Oetomo, and L. Feijs, "Monitoring body temperature of newborn infants at neonatal intensive care units using wearable sensors," in *Proc. 5th Int. Conf. Body Area Netw. (BodyNets)*, 2010, pp. 188–194, doi: 10.1145/2221924.2221960.

[11] S. Bouwstra, W. Chen, L. Feijs, and S. B. Oetomo, "Smart jacket design for neonatal monitoring with wearable sensors," in *Proc. 6th Int. Workshop Wearable Implant. Body Sensor Netw.*, Jun. 2009, pp. 162–167, doi: 10.1109/bsn.2009.40.

[12] Y. Rimet, Y. Brusquet, D. Ronayette, C. Dageville, M. Lubrano, E. Mallet, C. Rambaud, C. Terlaud, J. Silve, O. Lerda, L. I. Netchiporouk, and J.-L. Weber, "Surveillance of infants at risk of apparent life threatening events (ALTE) with the BBA bootee: A wearable multiparameter monitor," in *Proc. 29th Annu. Int. Conf. IEEE Eng. Med. Biol. Soc.*, Aug. 2007, pp. 4997–5000, doi: 10.1109/iembs.2007.4353462.

[13] S. Ramasamy and A. Balan, "Wearable sensors for ECG measurement: A review," *Sensor Rev.*, vol. 38, no. 4, pp. 412–419, Sep. 2018, doi: 10.1108/sr-06-2017-0110.

[14] J. Vertens, F. Fischer, C. Heyde, F. Hoeflinger, R. Zhang, L. Reindl, and A. Gollhofer, "Measuring respiration and heart rate using two acceleration sensors on a fully embedded platform," in *Proc. 3rd Int. Congr. Sport Sci. Res. Technol. Support*, 2015, pp. 15–23.

[15] T. S. Chadha, H. Watson, S. Birch, G. A. Jenouri, A. W. Schneider, M. A. Cohn, and M. A. Sackner, "Validation of respiratory inductive plethysmography using different calibration procedures," *Amer. Rev. Respiratory Disease*, vol. 125, no. 6, pp. 644–649, Jun. 1982, doi: 10.1164/arrd.1982.125.6.644.

[16] Z. Zhang, W. Wang, B. Wang, H. Wu, H. Liu, and Y. Zhang, "A prototype of wearable respiration biofeedback platform and its preliminary evaluation on cardiovascular variability," in *Proc. 3rd Int. Conf. Bioinf. Biomed. Eng.*, Jun. 2009, pp. 1–4, doi: 10.1109/icbbe.2009.5162230.

[17] D. Mack, D. Mack, J. Patrie, P. Suratt, R. Felder, and M. Alwan, "Development and preliminary validation of heart rate and breathing rate detection using a passive, ballistocardiography-based sleep monitoring system," *IEEE Trans. Inf. Technol. Biomed.*, vol. 13, no. 1, pp. 111–120, Jan. 2009, doi: 10.1109/titb.2008.2007194.

[18] C. Yang and N. Tavassolian, "Combined Seismo- and Gyro-cardiography: A more comprehensive evaluation of heart-induced chest vibrations," *IEEE J. Biomed. Health Inform.*, vol. 22, no. 5, pp. 1466–1475, Sep. 2018, doi: 10.1109/jbhi.2017.2764798.

[19] E. Piuzzi, A. Capuano, S. Pisa, P. Cappa, F. Patane, S. Rossi, N. Giaquinto, and G. M. D'aucelli, "Impedance plethysmography system with inertial measurement units for motion artefact reduction: Application to continuous breath activity monitoring," in *Proc. IEEE Int. Symp. Med. Meas. Appl. (MeMeA)*, May 2015, pp. 386–390, doi: 10.1109/memea.2015.7145233.

[20] S. Bao, S. Yin, H. Chen, and W. Chen, "A wearable multimode system with soft sensors for lower limb activity evaluation and rehabilitation," in *Proc. IEEE Int. Instrum. Meas. Technol. Conf. (I2MTC)*, May 2018, pp. 1–6, doi: 10.1109/i2mtc.2018.8409880.

[21] D. R. Nordli, C. W. Bazil, M. L. Scheuer, and T. A. Pedley, "Recognition and classification of seizures in infants," *Epilepsia*, vol. 38, no. 5, pp. 553–560, May 1997, doi: 10.1111/j.1528-1157.1997.tb01140.x.

[22] H. Chen, M. Xue, Z. Mei, S. Bambang Oetomo, and W. Chen, "A review of wearable sensor systems for monitoring body movements of neonates," *Sensors*, vol. 16, no. 12, p. 2134, Dec. 2016, doi: 10.3390/s16122134.

[23] J. Lockman, R. S. Fisher, and D. M. Olson, "Detection of seizure-like movements using a wrist accelerometer," *Epilepsy Behavior*, vol. 20, no. 4, pp. 638–641, Apr. 2011, doi: 10.1016/j.yebeh.2011.01.019.

[24] P.-W. Huang, C.-H. Hsieh, M.-C. Liang, C. Tsou, and S.-Y. Lee, "ECG monitoring and emotion stabilization system with a physiological information platform for drivers," in *Proc. Int. Symp. Bioelectron. Bioinf. (ISBB)*, Oct. 2015, pp. 180–183, doi: 10.1109/isbb.2015.7344953.

[25] F. AL-Khalidi, R. Saatchi, D. Burke, H. Elphick, and S. Tan, "Respiration rate monitoring methods: A review," *Pediatr. Pulmonol.*, vol. 46, no. 6, pp. 523–529, Jun. 2011, doi: 10.1002/ppul.21416.

[26] VTechAdmin. *Fabrics—Shieldex Trading*. Accessed: Nov. 21, 2019. [Online]. Available: https://www.shieldextrading.net/products/fabrics/

[27] T. Tamura and W. Chen, *Seamless Healthcare Monitoring: Advancements in Wearable, Attachable, and Invisible Devices*. Springer, 2018.

[28] B.-Y. Chang and S.-M. Park, "Electrochemical impedance spectroscopy," *Annu. Rev. Anal. Chem.*, vol. 3, pp. 207–229, Jul. 2010, doi: 10.1146/annurev.anchem.012809.102211.

[29] *Wearable Sensor Technology | Wireless IMU | ECG | EMG | GSR*. Accessed: Jul. 2, 2019. [Online]. Available: http://www.shimmersensing.com/

[30] J. Lee, K. Jeong, J. Yoon, and M. Lee, "A simple real-time QRS detection algorithm," in *Proc. 18th Annu. Int. Conf. IEEE Eng. Med. Biol. Soc.*, vol. 4, Oct./Nov. 1996, pp. 1396–1398, doi: 10.1109/iembs.1996.647473.

[31] A. J. Camm, "Heart rate variability: Standards of measurement, physiological interpretation, and clinical use. Task force of the European society of cardiology the north american society of pacing electrophysiology," *Circulation*, vol. 93, no. 5, pp. 1043–1065, 1996, doi: 10.1161/01.CIR.93.5.1043.

[32] D. P. Golden, R. A. Wolthuis, and G. W. Hoffler, "A spectral analysis of the normal resting electrocardiogram," *IEEE Trans. Biomed. Eng.*, vol. BME-20, no. 5, pp. 366–372, Sep. 1973, doi: 10.1109/tbme.1973.324231.

[33] O. Y. De Vel, "R-wave detection in the presence of muscle artifacts," *IEEE Trans. Biomed. Eng.*, vol. BME-31, no. 11, pp. 715–717, Nov. 1984, doi: 10.1109/tbme.1984.325395.

[34] G. Friesen, T. Jannett, M. Jadallah, S. Yates, S. Quint, and H. Nagle, "A comparison of the noise sensitivity of nine QRS detection algorithms," *IEEE Trans. Biomed. Eng.*, vol. 37, no. 1, pp. 85–98, 1st Quart., 1990, doi: 10.1109/10.43620.

[35] M. Merri, D. Farden, J. Mottley, and E. Titlebaum, "Sampling frequency of the electrocardiogram for spectral analysis of the heart rate variability," *IEEE Trans. Biomed. Eng.*, vol. 37, no. 1, pp. 99–106, 1st Quart., 1990, doi: 10.1109/10.43621.

HONGYU CHEN was born in Jiangxi, China, in 1989. He received the B.S. degree from Nanchang University, China, in 2012, and the M.S. degree from Zhejiang University, China, in 2015. He is currently pursuing the Ph.D. degree from the Eindhoven University of Technology, The Netherlands, all in industrial design. From 2016 to 2018, he was a Research Assistant with the Institute of Center for Intelligent Medical Electronics, Fudan University, Shanghai, China. His research interests include the wearable sensor design and neonatal monitoring with wearable sensor.

SHENJIE BAO received the B.S. degree in electronic engineering from Fudan University, Shanghai, China, in 2017. He is currently pursuing the M.S. degree in electronic and communication engineering with Fudan University, Shanghai. His research interests include wearable biomedical signal acquisition hardware system design, and development of software and algorithm for the signal processing to meet with the clinical requirements. He also has experience in data analyzing and collaborates closely with industry.

CHUNMEI LU received the B.S. degree in nursing from Shanghai Jiao Tong University, in 2014. She is currently working with the Department of Neonates, Children s Hospital of Fudan University, as a Head Nurse. She has nearly 25 years of research experience in the fields of neonatal nursing management, neonatal vascular pathway management, early intervention, and follow-up of brain development in high-risk infants. So far, she has participated in the preparation of two books and published more than ten articles. Among them, "Application of key treatment techniques based on NIDCAP Theory in Nursing of premature infants" received the Second Prize of Science and Technology Award from Chinese Nursing Association.

LAISHUAN WANG received the B.S. and M.S. degrees in medicine from Zhengzhou University, China, in 2000, and the M.D. degree in medicine from Fudan University, Shanghai, China, in 2003. He is currently a Full Professor with the Department of Electronic Engineering, Fudan University. He is also a Full Professor and the Deputy Director of the Department of Neonatology, Children's Hospital of Fudan University. He is currently the Deputy Chairman of the Neonatology Group, Chinese Academy of Pediatrics, the Deputy Chairman of the Neurology Group, Neonatology Branch, Chinese Medical Association, and a member of the Neonatology Group, Shanghai Pediatric Society.

JIANHUA MA received the B.S. and Ph.D. degrees in materials science and engineering from the Beijing University of Chemical Technology, Beijing, China, in 2013. From 2017 to 2019, he held a postdoctoral position at the Department of Macromolecular Science, Fudan University, Shanghai, China. He is currently an Associate Professor with Xi'an Polytechnic University, Xi'an, China. His research interest includes preparation of intelligent wearable devices with new carbon materials, such as graphene.

PENG WANG was born in Chongqing, China, in 1992. He received the B.S. degree in polymer materials and engineering from Sichuan University, in 2014, and the Ph.D. degree in polymer chemistry and physics from Fudan University, in 2019. His research interests include preparation and application of graphene sheets, graphene-based polymer composites, and smart sensors.

HONGBIN LU received the B.S. and M.S. degrees in fine chemical from the Beijing Institute of Technology, and the Ph.D. degree in macromolecule chemistry and physics from the Changchun Institute of Applied Chemistry, Chinese Academy of Science, in 1999. Then, he held a postdoctoral position at Fudan University, from 2000 to 2001, and the University of Southern California, from 2001 to 2004, before joining Fudan University, in 2004. He is currently a Professor with the Department of Macromolecular Science and the State Key Laboratory of Molecular Engineering of Polymers. His researches focus on production of varied graphene materials and their application in multiple fields, especially in energy storage materials, polymer composites, catalysts, and heat interfacial materials. He is the author of more than 70 articles and more than 40 inventions.

FENG SHU received the B.E. degree from Shanghai Jiao Tong University, China, in 2002, the M.Eng. degree from Nanyang Technological University, Singapore, in 2004, and the Ph.D. degree from The University of Melbourne, Australia, in 2007, all in electrical engineering. Since graduation, he has held various research and development positions in the microelectronics field at the Holst Center and at ASML, The Netherlands. He has been with Fudan University, China, as a Faculty Member. His research interests include high performance embedded computing, advanced sensor algorithms, and systems for industrial applications.

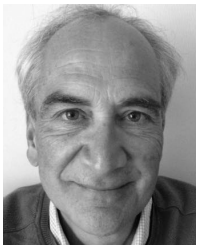

SIDARTO BAMBANG OETOMO was born in 1951. He was trained and worked in pediatrics and neonatology at the Beatrix Children's Hospital, University of Groningen, The Netherlands, more than 20 years. He research was focused on neonatal lung disease and surfactant. In 1988, he spend a year at the Perinatal Research Laboratories, University of California, Torrance. He was appointed as a Professor of neonatology, in 1996. In 2003, he moved to Veldhoven, where he worked as a Neonatologist at Máxima Medical Center. In 2007, he was appointed as a Professor of industrial design at the Eindhoven University of Technology. The topic of his research is to design technologies to reduce pain and stress for newborn babies and to promote the bonding of mother and his child.

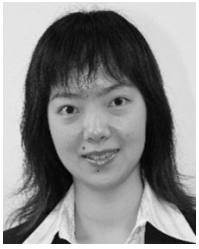

WEI CHEN (Senior Member, IEEE) received the B.S. and M.S. degrees from Xi'an Jiaotong University, in 1999 and 2002, respectively, and the Ph.D. degree from The University of Melbourne, in 2007. From 2008 to 2015, she was an Assistant Professor with the Department of Industrial Design, Technical University of Eindhoven. She is currently a Full Professor with the Department of Electronic Engineering, Fudan University. Her research interests include wearable sensor systems, biomedical signal processing, and health monitoring. She is a Regional Representative of the IEEE EMBS Technical Committee on Wearable Biomedical Sensors and Systems and the Vice Chair of the IEEE Sensors and Systems Council. She is also an Associate Editor of the IEEE JOURNAL OF BIOMEDICAL HEALTH INFORMATICS (JBHI).